Efficient Concatenated Bosonic Code for Additive Gaussian Noise

Kosuke Fukui[1] Takaya Matsuura,[2] and Nicolas C. Menicucci[2]

[1]*Department of Applied Physics, School of Engineering, The University of Tokyo,*
7-3-1 Hongo, Bunkyo-ku, Tokyo 113-8656, Japan
[2]*Centre for Quantum Computation and Communication Technology, School of Science, RMIT University,*
Melbourne, Victoria 3000, Australia

Bosonic codes offer noise resilience for quantum information processing. Good performance often comes at a price of complex decoding schemes, limiting their practicality. Here, we propose using a Gottesman-Kitaev-Preskill code to detect and discard error-prone qubits, concatenated with a quantum parity code to handle the residual errors. Our method employs a simple linear-time decoder that nevertheless offers significant performance improvements over the standard decoder. Our Letter may have applications in a wide range of quantum computation and communication scenarios.

Introduction.—Quantum-error-correcting codes known as bosonic codes [1] protect discrete quantum information encoded in bosonic mode(s). The infinite-dimensional nature of the bosonic Hilbert space allows more sophisticated encoding than the conventional single-photon encoding [2–4] or matter-based qubits [5–7]. Various codes exist that protect encoded quantum information against decoherence, with better than break-even performance demonstrated recently [8,9]. These versatile codes find applications in optical, solid-state, and vibrational systems. We call qubits encoded in a bosonic code "bosonic qubits."

While quantum supremacy has been demonstrated in both solid-state qubits [10] and optics [11,12], the ultimate goal of a large-scale, fault-tolerant quantum computer will require additional innovations, and its ultimate architecture remains an open question. Such requirements on the device can be roughly classified into scalability (many qubits) and fault tolerance (of good quality) [13] and architectures designed to use bosonic qubits, as the information carriers have recently demonstrated prominent advances in both areas.

Progress on scalability has been most significant in optics through demonstrations of computationally universal continuous-variable (CV) cluster states [14,15] comprising $\sim 10^4$ modes [16,17] and measurement-based implementation of CV quantum gates [18,19]. When used to process the bosonic qubits proposed by Gottesman, Kitaev, and Preskill (GKP) [20]—and with high enough squeezing—these architectures can be made fault tolerant [21,22].

The GKP qubit [20] has emerged as a promising bosonic qubit for fault tolerance due to its excellent performance against common types of noise [1]. Experiments involving trapped ions [23,24] and superconducting circuits [25,26] have demonstrated a GKP qubit, with the latter boasting a squeezing level close to 10 dB. This level is sufficient for

fault tolerance in some proposed architectures [27,28] and is approaching what is required by others [29–31]. Numerous proposals exist to produce these states in optics as well [32–45]. Furthermore, the GKP qubit performs well for quantum communication [46–48] thanks to the robustness against photon loss [1]. In fact, recent results show that using GKP qubits may greatly enhance long-distance quantum communication [49,50].

A conventional noise model in bosonic systems is the Gaussian quantum channel (GQC) [20,51], also known as additive Gaussian noise. While the landscape of Gaussian operations includes other types of channels [52,53], the GQC is a particularly common one [54], and we focus on it here. The GQC is a simple canonical type of noise for analyzing bosonic code performance [20,51]. Buoyed by the fact that displacements form an operator basis, protecting against the GQC allows some level of protection against all types of bosonic noise [20]. The GKP encoding is specifically designed to protect qubit information against the GQC (and thus against bosonic noise in general), but despite this, its performance "out of the box" as a single-mode code is suboptimal against the GQC [20,51].

A long-standing open problem in CV quantum information [51] is to design a simple and efficient concatenated code that enables finite-rate quantum communication with levels of GQC noise that are guaranteed to allow this [51,55]. This bound can be achieved by GKP-type codes based on high-dimensional sphere packing [51], but the authors of that work were unsatisfied with this because such a code is not concatenated and thus offers no obvious structure that might be exploited [56,57] to further improve its performance.

Analog quantum error correction (QEC) [58] makes strides toward achieving the goal of Ref. [51] by using the

real-valued syndrome of a GKP qubit to improve error recovery in a concatenated code by selecting the most likely error pattern for a given syndrome. In fact, when used with a suitable qubit code, analog QEC can achieve the bound [27,58]. This would seem to be the end of the story, except for one major drawback: The decoder for analog QEC employs a type of belief propagation [59] that may become unwieldy in real-world implementations. This is especially true in optical architectures, where fast processing of the outcomes is vital [29,30]. In such cases—and especially when hardware-level control is used—reducing the number of bits required to represent outcomes may be critical to fast decoding.

What we would like instead is a simple CV-level decoder that generates discrete outcomes that can be fed directly into a qubit-level code at the next level of concatenation. This is the key innovation that makes further improvements feasible, since more complicated codes or additional layers of concatenation do not require modifying the CV-level decoding scheme, thus keeping the decoder simple and efficient.

In this Letter, we make significant progress toward achieving this goal. Our innovation uses the CV-level measurement outcome from GKP error correction merely to decide whether to keep the qubit or discard it entirely and treat it as a located erasure error. This is a simple local decoding step and does not require complicated modeling of CV-level errors. The quantum parity code (QPC) [60] is well suited to dealing with the discarded qubits [61–63], and we numerically show that concatenating the GKP code with a QPC considerably improves its performances with a small code and straightforward decoding, linear in the number of modes.

GKP qubit.—The GKP code encodes a qubit in an oscillator in a way that protects against errors caused by small displacements in the q (position) and p (momentum) quadratures [20]. [We use conventions $a = (q + ip)/\sqrt{2}$, $[q, p] = i$, $\hbar = 1$, vacuum variance $= 1/2$.] The ideal code states of the GKP code are Dirac combs in q and in p. Physical states are finitely squeezed approximations to these and are often modeled as a comb of Gaussian peaks of width (i.e., observable standard deviation) σ, with separation $\sqrt{\pi}$, and modulated by a larger Gaussian envelope of width $1/\sigma$. Since these approximate states are not orthogonal, there is a probability of misidentifying $|0\rangle$ as $|1\rangle$ (and vice versa) in a measurement of logical Z, which is implemented by a q measurement and binning to the nearest integer multiple of $\sqrt{\pi}$. Similarly, $|+\rangle$ and $|-\rangle$ may be misidentified when measuring logical X with a p measurement. A qubit-level measurement error occurs when the measured outcome is more than $\sqrt{\pi}/2$ away from the correct outcome.

Gaussian quantum channel.—The GKP code is tailored to combat the GQC, which randomly displaces the state in phase space according to a Gaussian distribution [20,51].

The GQC is described by the superoperator $\mathcal{G}_\xi$ acting on density operator ρ as

$$\mathcal{G}_\xi(\rho) = \frac{1}{\pi\xi^2} \int d^2\alpha \, e^{-|\alpha|^2/\xi^2} D(\alpha)\rho D(\alpha)^\dagger, \qquad (1)$$

where $D(\alpha) = e^{\alpha a^\dagger - \alpha^* a}$ is the phase-space displacement operator. With $\alpha = (1/\sqrt{2})(u + iv)$, the position q and momentum p are displaced independently as $q \to q + u$, $p \to p + v$, where u and v are real Gaussian random variables with mean zero and variance ξ^2. Therefore, the GQC maintains the locations of the Gaussian peaks in the probability for the measurement outcome, but it increases the variance of each spike by ξ^2 in both quadratures.

Noise model.—GKP error correction, in both its original [20] (Steane-style [64]) form and in its teleportation-based [65] (Knill-style [66]) form, involve measuring the deviation of the state's support in each quadrature (q, p) away from an integer multiple of $\sqrt{\pi}$. These measurement outcomes—each of the form $s_m = n\sqrt{\pi} + \Delta_m$ with integer n and $|\Delta_m| \leq \sqrt{\pi}/2$, where even and odd n correspond to 0 and 1 logical bit values, respectively—together form the syndrome. Normally, each value of Δ_m locally determines the displacement to apply in order to correct the error—either snapping back to grid in the original method [20] or applying a logical Pauli in the teleportation-based method [65]. Analog QEC [27,58] instead feeds all these real-valued syndrome data s_m directly to a higher-level decoder, which makes a global decision. Our proposal keeps aspects of both approaches. We use Δ_m to locally decide whether we keep it or give up and report the qubit as lost to the next-level decoder.

We model a damaged GKP code word as an ideal one [20] that has been displaced by a definite (but unknown) amount in each quadrature. This approximately models the errors due to both coherent and incoherent noise [21,27,58,67] and simplifies the analysis. Because of the $2\sqrt{\pi}$ periodicity of all GKP code words, given any initial distribution $p_0(u)$ of the unknown displacement u in a single quadrature, its effect on a GKP code word is captured by folding $p_0(u)$ into the *wrapped* distribution $p(u) = \sum_{k \in \mathbb{Z}} p_0(u + 2k\sqrt{\pi})$, whose domain is $[-\sqrt{\pi}, \sqrt{\pi})$. When p_0 is a zero-mean Gaussian of variance σ^2, it wraps into

$$p(u) = \frac{1}{2\sqrt{\pi}} \vartheta\left(-\frac{u}{2\sqrt{\pi}}, \frac{i\sigma^2}{2}\right), \qquad (2)$$

where $\vartheta(z, \tau) = \sum_{m \in \mathbb{Z}} \exp[2\pi i(\frac{1}{2}m^2\tau + mz)]$ is a Jacobi theta function of the third kind. Figure 1(a) shows this distribution and the logical effect of a shift by u (mod $2\sqrt{\pi}$) on measuring a GKP code word.

Highly reliable measurement.—Logical errors occur when the GKP syndrome value s_m, which is wrapped mod $\sqrt{\pi}$, misidentifies u as $u \pm \sqrt{\pi}$ [20]. The highly
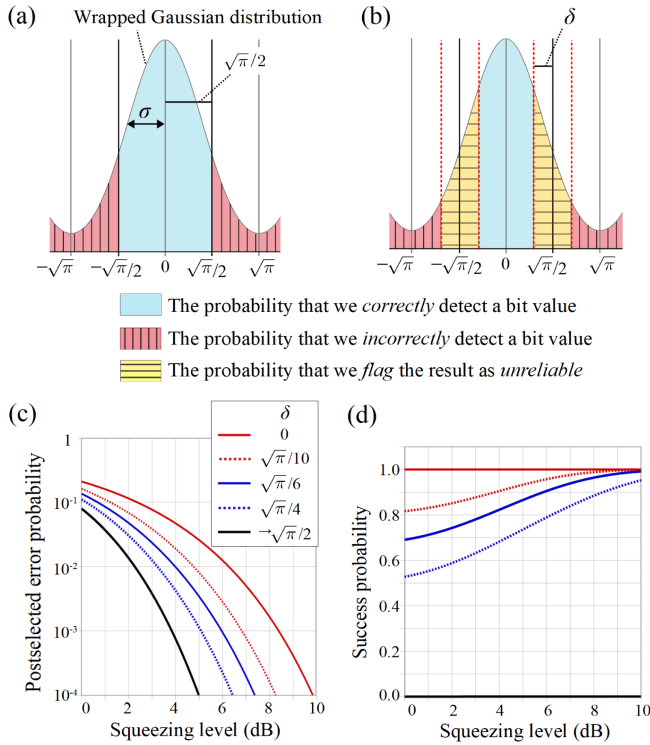
FIG. 1. Effect of additive Gaussian noise [67] on measuring a GKP qubit. (a) Effect of shift by u (mod $2\sqrt{\pi}$), distributed according to $p(u)$ in Eq. (2), on an ordinary measurement of a GKP qubit [20]. (b) The highly reliable measurement [27] flags outcomes in the 2δ-wide "danger zone" (yellow) as unreliable. (c) Postselected error probability of the HRM for several values of δ. (d) Corresponding success probability. Note: (squeezing level in decibels) $= -10\log_{10}(\sigma^2/\sigma_{\rm vac}^2)$, where the vacuum variance $\sigma_{\rm vac}^2 = \frac{1}{2}$.

reliable measurement (HRM) [27] buffers against this possibility by introducing a danger zone of outcomes $0 \le \sqrt{\pi}/2 - |\Delta_{\rm m}| < \delta$ for some $\delta > 0$. Outcomes in this zone are flagged as unreliable, with $\delta \to 0$ recovering the usual case [20]. This corresponds to flagging as unreliable any displacement u (mod $2\sqrt{\pi}$) that falls within δ of a crossover point $\pm\sqrt{\pi}/2$, as shown in Fig. 1(b). When the HRM flags a result $s_{\rm m}$ as unreliable, the corresponding qubit is discarded and treated as a located erasure error $(s_{\rm m} \to E)$, while otherwise the result is kept and binned as usual $(s_{\rm m} \to \pm 1)$ [20] depending on which of an even or odd multiple of $\sqrt{\pi}$ $s_{\rm m}$ is close to. The HRM is thus a ternary (three-outcome) decoder for GKP qubits that maps each raw CV outcome $s_{\rm m}$ from $\mathbb{R} \to \{\pm 1, E\}$.

Given a definite displacement $u \in [-\sqrt{\pi}, \sqrt{\pi})$, we define probabilities for three cases: the measurement result is correct, $P^{(c)} = \Pr(|u| < \sqrt{\pi}/2 - \delta)$; the result is incorrect, $P^{(i)} = \Pr(|u| > \sqrt{\pi}/2 + \delta)$; or the result is unreliable and the qubit discarded, $P^{(d)} = \Pr(-\delta < |u| - \sqrt{\pi}/2 < \delta)$. We further define the "success probability," $1 - P^{(d)}$, as the probability the qubit was not discarded and the
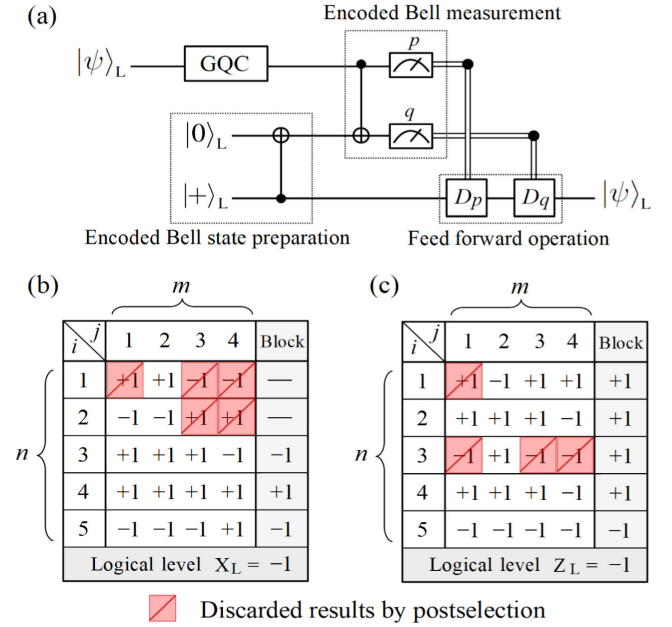

FIG. 2. Trading errors for loss to improve error correction. (a) Teleportation-based QEC using GKP qubits [20] concatenated with the QPC [60,61]. All gates are shown at the GKP logical level. The feed forward operations D_p and D_q implement logical-level X and Z operations via physical-level displacements [20], determined by the outcomes of the logical Bell measurement [61]. (b) Encoded measurement with the (5,4) QPC in the X basis. Performing the HRM in p [Fig. 1(b)] gives, for each qubit, either a binary outcome (± 1) or a located erasure error (E). The latter is indicated in red (with the unreliable binary outcome underneath) and occurs when the CV-level outcome is in the danger zone (see Fig. 1). A horizontal block is ignored if it has any discarded outcomes. All remaining blocks have their parity (product) taken, after which a majority vote of those parities determines the logical outcome—with heralded failure if there is no majority. (c) Encoded measurement with the (5,4) QPC in the Z basis. This is similar to (b), but with the HRM done in q and majority voting within a block preceding taking the parity of the blocks' voting outcomes—with heralded failure if any block has no majority [61]. (See the Supplemental Material [68] for further details.) Without the HRM, both logical outcomes would have been incorrect (likely due to uncorrected errors in the discarded values).

"postselected error probability," $P_{\rm post}^{(i)} = P^{(i)}/(1 - P^{(d)})$, as the probability of getting an incorrect outcome within the sample of qubits that are not discarded. Decreasing the postselected error probability (by increasing δ) reduces the success probability [27], as shown in Figs. 1(c) and 1(d).

Trading errors for loss.—The HRM is the key to improving the performance of the code against the GQC without the significant computational overhead required for conventional analog QEC for this code. Analog QEC for this code requires modeling the joint likelihood of real-valued outcomes over multimode code words, which will be intractable when the code size gets larger, while the

HRM maps *locally detected* unreliable results to lost qubits at known locations.

Loss-tolerant QEC codes were originally proposed to overcome loss of individual photons—the main hurdle in quantum computation based on a single-photon qubit. Here, concatenating GKP qubits with one of these codes compensates for the discarded ("lost") qubits due to using the HRM. This trade of unlocated errors for located erasures makes the logical qubit more robust. In the following, we concatenate GKP qubits with the QPC proposed by Ralph *et al.* [60] and implement teleportation-based QEC as proposed by Muralidharan *et al.* [61].

The (n, m) QPC [61] is an nm-qubit code built from n blocks of m qubits. Logical basis states are $|\pm\rangle_{\mathrm{L}} = 2^{-n/2}(|0\rangle^{\otimes m} \pm |1\rangle^{\otimes m})^{\otimes n}$. In our code, the physical qubit states are square-lattice GKP states [20] of a single bosonic mode—i.e., $|0\rangle = |0_{\mathrm{GKP}}\rangle$ and $|1\rangle = |1_{\mathrm{GKP}}\rangle$.

We analyze the performance of our code by simulating the process shown in Fig. 2, which implements error correction using the teleportation-based protocol of Ref. [61] (see figure caption and the Supplemental Material [68] for details). Using teleportation guarantees that the output state is already in the logical subspace, and only logical corrections are required [66].

Numerical simulation.—We evaluate our proposed QEC method using a Monte Carlo simulation of the circuit in Fig. 2(a). The input state passes through a GQC [Eq. (1)]. Our model simulates code-capacity noise (i.e., assuming no errors aside from the channel noise itself [69,70]) in order to evaluate the best possible performance of our code under the GQC and to compare with previous results [20,27,51,58]. We consider two cases: (a) the conventional case, which corresponds to choosing $\delta_X = \delta_Z = 0$, and (b) an optimized choice of δ_X and δ_Z for logical X and Z errors (specified below).

We define the "failure probability" of the QPC as the probability that the final value of X_{L} or Z_{L} is wrong. When a heralded failure occurs—see caption of Figs. 2(b) and 2(c)—we randomly assign the outcome. (More sophisticated handling may be possible, e.g., concatenating with a higher-level code.)

Figure 3 shows the performance of (a) the QPC without HRM and (b) that with HRM, as a function of the standard deviation of the GKP qubit for several sizes (n, m) of the QPC. In Fig. 3(a), we optimized the value of n for the given m so that the failure probability is minimized; in Fig. 3(b), we optimized δ_Z and δ_X, as well as n, so that the failure probability is minimized. For $m = 5, 7, 9, 11, 13$, respectively, the optimized values of n are $n = 13, 39, 109, 209, 817$ for the conventional method (a) and $n = 13, 39, 117, 337, 967$ for our new method (b). Furthermore, the optimized values of the HRM parameters δ_X and δ_Z for (b) are $\delta_X/\sqrt{\pi} = 0.0963, 0.0967, 0.0968, 0.0968$, and 0.0968 and $\delta_Z/\sqrt{\pi} = 0.130, 0.134, 0.137, 0.138$, and 0.139, respectively, which leads to the loss probability of
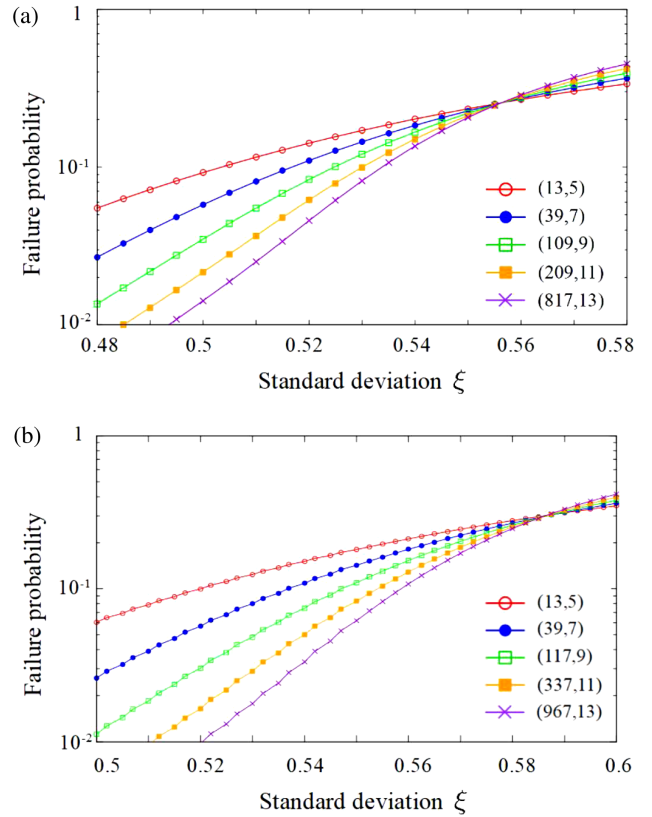

FIG. 3. Failure probabilities using the (n, m) QPC, as shown in Fig. 2, for (a) $\delta_X = \delta_Z = 0$ (conventional GKP error correction [20]) and (b) optimized values of the HRM parameters δ_X and δ_Z shown in the main text.

about 15% for X and 21%–22% for Z. The conventional method (a) gives a threshold of $\xi \approx 0.555$, matching previous work with concatenated codes and simple decoding [20,51]. Our improved method greatly surpasses this, achieving a threshold $\xi \approx 0.585$ with a simple and efficient decoder.

Conclusion.—The key insight of this Letter is that one does not need to model the full likelihood function [27,58] to correctly interpret GKP syndrome information [20] within a concatenated code. Instead, the real-valued outcomes can be coarse grained to one of three qubit-level outcomes through the HRM mapping $\mathbb{R} \rightarrow \{\pm 1, E\}$, where E represents an untrustworthy value. These ternary outcomes suffice to achieve a considerable improvement of the code against GQC by treating E outcomes as erasure errors and concatenating with a qubit-level code designed to handle such errors [60–63].

The innovation of this Letter over using the full analog information for error correction [27,58] lies in the efficiency and versatility of the decoder. Respectively, (1) decoding happens in linear time since the CV-level decoding is entirely local; and (2) the HRM wraps each GKP qubit in a simple error-detecting code, so concatenating with any qubit-level code designed to handle

erasures [71–73] should benefit from this type of outcome mapping. Further applications and extensions include improved decoding in GKP-based architectures (e.g., [29–31]) and in codes that exploit biased noise (e.g., [70,74–76]). The numerical result implies that there is room for further improvement to achieve the hashing bound of the GQC, $\xi \approx 0.607$, by using more complicated codes, additional layers of concatenation, or sophisticated decoders. Our innovation, however, is rooted in the simple and efficient decoder.

[1] V. V. Albert, K. Noh, K. Duivenvoorden, D. J. Young, R. Brierley, P. Reinhold, C. Vuillot, L. Li, C. Shen, S. Girvin *et al.*, Performance and structure of single-mode bosonic codes, Phys. Rev. A **97**, 032346 (2018).

[2] E. Knill, R. Laflamme, and G. J. Milburn, A scheme for efficient quantum computation with linear optics, Nature (London) **409**, 46 (2001).

[3] P. Kok, W. J. Munro, K. Nemoto, T. C. Ralph, J. P. Dowling, and G. J. Milburn, Linear optical quantum computing with photonic qubits, Rev. Mod. Phys. **79**, 135 (2007).

[4] T. Rudolph, Why I am optimistic about the silicon-photonic route to quantum computing, APL Photonics **2**, 030901 (2017).

[5] M. Kjaergaard, M. E. Schwartz, J. Braumüller, P. Krantz, J. I.-J. Wang, S. Gustavsson, and W. D. Oliver, Superconducting qubits: Current state of play, Annu. Rev. Condens. Matter Phys. **11**, 369 (2020).

[6] J. Koch, T. M. Yu, J. Gambetta, A. A. Houck, D. Schuster, J. Majer, A. Blais, M. H. Devoret, S. M. Girvin, and R. J. Schoelkopf, Charge-insensitive qubit design derived from the Cooper pair box, Phys. Rev. A **76**, 042319 (2007).

[7] J. A. Schreier, A. A. Houck, J. Koch, D. I. Schuster, B. R. Johnson, J. M. Chow, J. M. Gambetta, J. Majer, L. Frunzio, M. H. Devoret *et al.*, Suppressing charge noise decoherence in superconducting charge qubits, Phys. Rev. B **77**, 180502(R) (2008).

[8] N. Ofek, A. Petrenko, R. Heeres, P. Reinhold, Z. Leghtas, B. Vlastakis, Y. Liu, L. Frunzio, S. Girvin, L. Jiang *et al.*, Extending the lifetime of a quantum bit with error correction in superconducting circuits, Nature (London) **536**, 441 (2016).

[9] L. Hu, Y. Ma, W. Cai, X. Mu, Y. Xu, W. Wang, Y. Wu, H. Wang, Y. Song, C.-L. Zou *et al.*, Quantum error correction and universal gate set operation on a binomial bosonic logical qubit, Nat. Phys. **15**, 503 (2019).

[10] F. Arute, K. Arya, R. Babbush, D. Bacon, J. C. Bardin, R. Barends, R. Biswas, S. Boixo, F. G. Brandao, D. A. Buell *et al.*, Quantum supremacy using a programmable superconducting processor, Nature (London) **574**, 505 (2019).

[11] H.-S. Zhong, H. Wang, Y.-H. Deng, M.-C. Chen, L.-C. Peng, Y.-H. Luo, J. Qin, D. Wu, X. Ding, Y. Hu *et al.*, Quantum computational advantage using photons, Science **370**, 1460 (2020).

[12] L. S. Madsen, F. Laudenbach, M. F. Askarani, F. Rortais, T. Vincent, J. F. Bulmer, F. M. Miatto, L. Neuhaus, L. G. Helt, M. J. Collins *et al.*, Quantum computational advantage with a programmable photonic processor, Nature (London) **606**, 75 (2022).

[13] D. P. DiVincenzo, The physical implementation of quantum computation, Fortschr. Phys. **48**, 771 (2000).

[14] N. C. Menicucci, P. van Loock, M. Gu, C. Weedbrook, T. C. Ralph, and M. A. Nielsen, Universal Quantum Computation with Continuous-Variable Cluster States, Phys. Rev. Lett. **97**, 110501 (2006).

[15] N. C. Menicucci, Temporal-mode continuous-variable cluster states using linear optics, Phys. Rev. A **83**, 062314 (2011).

[16] W. Asavanant, Y. Shiozawa, S. Yokoyama, B. Charoensombutamon, H. Emura, R. N. Alexander, S. Takeda, J.-i. Yoshikawa, N. C. Menicucci, H. Yonezawa *et al.*, Generation of time-domain-multiplexed two-dimensional cluster state, Science **366**, 373 (2019).

[17] M. V. Larsen, X. Guo, C. R. Breum, J. S. Neergaard-Nielsen, and U. L. Andersen, Deterministic generation of a two-dimensional cluster state, Science **366**, 369 (2019).

[18] W. Asavanant, B. Charoensombutamon, S. Yokoyama, T. Ebihara, T. Nakamura, R. N. Alexander, M. Endo, J.-i. Yoshikawa, N. C. Menicucci, H. Yonezawa, and A. Furusawa, Time-Domain-Multiplexed Measurement-Based Quantum Operations with 25-MHz Clock Frequency, Phys. Rev. Appl. **16**, 034005 (2021).

[19] M. V. Larsen, X. Guo, C. R. Breum, J. S. Neergaard-Nielsen, and U. L. Andersen, Deterministic multi-mode gates on a scalable photonic quantum computing platform, Nat. Phys. **17**, 1018 (2021).

[20] D. Gottesman, A. Kitaev, and J. Preskill, Encoding a qubit in an oscillator, Phys. Rev. A **64**, 012310 (2001).

[21] N. C. Menicucci, Fault-Tolerant Measurement-Based Quantum Computing with Continuous-Variable Cluster States, Phys. Rev. Lett. **112**, 120504 (2014).

[22] B. W. Walshe, L. J. Mensen, B. Q. Baragiola, and N. C. Menicucci, Robust fault tolerance for continuous-variable cluster states with excess antisqueezing, Phys. Rev. A **100**, 010301(R) (2019).

[23] C. Flühmann, T. L. Nguyen, M. Marinelli, V. Negnevitsky, K. Mehta, and J. P. Home, Encoding a qubit in a trapped-ion mechanical oscillator, Nature (London) **566**, 513 (2019).

[24] B. de Neeve, T.-L. Nguyen, T. Behrle, and J. P. Home, Error correction of a logical grid state qubit by dissipative pumping, Nat. Phys. **18**, 296 (2022).

[25] P. Campagne-Ibarcq, A. Eickbusch, S. Touzard, E. Zalys-Geller, N. E. Frattini, V. V. Sivak, P. Reinhold, S. Puri, S. Shankar, R. J. Schoelkopf *et al.*, Quantum error correction of a qubit encoded in grid states of an oscillator, Nature (London) **584**, 368 (2020).

[26] V. V. Sivak, A. Eickbusch, B. Royer, S. Singh, I. Tsioutsios, S. Ganjam, A. Miano, B. L. Brock, A. Z. Ding, L. Frunzio, S. M. Girvin, R. J. Schoelkopf, and M. H. Devoret, Real-time quantum error correction beyond break-even, Nature (London) **616**, 50 (2023).

[27] K. Fukui, A. Tomita, A. Okamoto, and K. Fujii, High-Threshold Fault-Tolerant Quantum Computation with Analog Quantum Error Correction, Phys. Rev. X **8**, 021054 (2018).

[28] K. Fukui, High-threshold fault-tolerant quantum computation with the GottesmanKitaev-Preskill qubit under noise in an optical setup, Phys. Rev. A **107**, 052414 (2023).

[29] J. E. Bourassa, R. N. Alexander, M. Vasmer, A. Patil, I. Tzitrin, T. Matsuura, D. Su, B. Q. Baragiola, S. Guha, G. Dauphinais, K. K. Sabapathy, N. C. Menicucci, and I. Dhand, Blueprint for a scalable photonic fault-tolerant quantum computer, Quantum **5**, 392 (2021).

[30] I. Tzitrin, T. Matsuura, R. N. Alexander, G. Dauphinais, J. E. Bourassa, K. K. Sabapathy, N. C. Menicucci, and I. Dhand, Fault-tolerant quantum computation with static linear optics, PRX Quantum **2**, 040353 (2021).

[31] M. V. Larsen, C. Chamberland, K. Noh, J. S. Neergaard-Nielsen, and U. L. Andersen, Fault-tolerant continuous-variable measurement-based quantum computation architecture, PRX Quantum **2**, 030325 (2021).

[32] S. Pirandola, S. Mancini, D. Vitali, and P. Tombesi, Constructing finite-dimensional codes with optical continuous variables, Europhys. Lett. **68**, 323 (2004).

[33] S. Pirandola, S. Mancini, D. Vitali, and P. Tombesi, Continuous variable encoding by ponderomotive interaction, Eur. Phys. J. D **37**, 283 (2006).

[34] S. Pirandola, S. Mancini, D. Vitali, and P. Tombesi, Generating continuous variable quantum codewords in the near-field atomic lithography, J. Phys. B **39**, 997 (2006).

[35] K. R. Motes, B. Q. Baragiola, A. Gilchrist, and N. C. Menicucci, Encoding qubits into oscillators with atomic ensembles and squeezed light, Phys. Rev. A **95**, 053819 (2017).

[36] M. Eaton, R. Nehra, and O. Pfister, Non-Gaussian and Gottesman–Kitaev–Preskill state preparation by photon catalysis, New J. Phys. **21**, 113034 (2019).

[37] D. Su, C. R. Myers, and K. K. Sabapathy, Conversion of Gaussian states to non-Gaussian states using photon-number-resolving detectors, Phys. Rev. A **100**, 052301 (2019).

[38] J. M. Arrazola, T. R. Bromley, J. Izaac, C. R. Myers, K. Brádler, and N. Killoran, Machine learning method for state preparation and gate synthesis on photonic quantum computers, Quantum Sci. Technol. **4**, 024004 (2019).

[39] I. Tzitrin, J. E. Bourassa, N. C. Menicucci, and K. K. Sabapathy, Progress towards practical qubit computation using approximate Gottesman-Kitaev-Preskill codes, Phys. Rev. A **101**, 032315 (2020).

[40] C.-Y. Lin, W.-C. Su, and S.-T. Wu, Encoding qubits into harmonic-oscillator modes via quantum walks in phase space, Quantum Inf. Process. **19**, 1 (2020).

[41] J. Hastrup and U. L. Andersen, Protocol for Generating Optical Gottesman-Kitaev-Preskill States with Cavity QED, Phys. Rev. Lett. **128**, 170503 (2022).

[42] K. Fukui, M. Endo, W. Asavanant, A. Sakaguchi, J. I. Yoshikawa, and A. Furusawa, Generating the Gottesman-Kitaev-Preskill qubit using a cross-Kerr interaction between squeezed light and Fock states in optics, Phys. Rev. A **105**, 022436 (2022).

[43] K. Fukui, S. Takeda, M. Endo, W. Asavanant, J.-i. Yoshikawa, P. van Loock, and A. Furusawa, Efficient Backcasting Search for Optical Quantum State Synthesis, Phys. Rev. Lett. **128**, 240503 (2022).

[44] K. Takase, K. Fukui, A. Kawasaki, W. Asavanant, M. Endo, J. Yoshikawa, P. van Loock, and A. Furusawa, Gaussian breeding for encoding a qubit in propagating light, arXiv:2212.05436.

[45] R. Yanagimoto, R. Nehra, R. Hamerly, E. Ng, A. Marandi, and H. Mabuchi, Quantum nondemolition measurements with optical parametric amplifiers for ultrafast universal quantum information processing, PRX Quantum **4**, 010333 (2023).

[46] C. H. Bennett and G. Brassard, Quantum cryptography: Public key distribution and coin tossing, Theor. Comput. Sci. **560**, 7 (2014).

[47] H.-J. Briegel, W. Dür, J. I. Cirac, and P. Zoller, Quantum Repeaters: The Role of Imperfect Local Operations in Quantum Communication, Phys. Rev. Lett. **81**, 5932 (1998).

[48] H. J. Kimble, The quantum internet, Nature (London) **453**, 1023 (2008).

[49] K. Fukui, R. N. Alexander, and P. van Loock, All-optical long-distance quantum communication with Gottesman-Kitaev-Preskill qubits, Phys. Rev. Res. **3**, 033118 (2021).

[50] F. Rozpędek, K. Noh, Q. Xu, S. Guha, and L. Jiang, Quantum repeaters based on concatenated bosonic and discrete-variable quantum codes, npj Quantum Inf. **7**, 102 (2021).

[51] J. Harrington and J. Preskill, Achievable rates for the Gaussian quantum channel, Phys. Rev. A **64**, 062301 (2001).

[52] F. Caruso, V. Giovannetti, and A. S. Holevo, One-mode bosonic Gaussian channels: A full weak-degradability classification, New J. Phys. **8**, 310 (2006).

[53] A. S. Holevo, One-mode quantum Gaussian channels: Structure and quantum capacity, Probl. Inf. Transm. **43**, 1 (2007).

[54] J. Eisert and M. M. Wolf, Gaussian Quantum Channels, in *Quantum Information with Continuous Variables of Atoms and Light* (World Scientific, London, 2007), pp. 23–42.

[55] A. S. Holevo and R. F. Werner, Evaluating capacities of bosonic Gaussian channels, Phys. Rev. A **63**, 032312 (2001).

[56] P. W. Shor and J. A. Smolin, Quantum error-correcting codes need not completely reveal the error syndrome, arXiv:quant-ph/9604006.

[57] D. P. DiVincenzo, P. W. Shor, and J. A. Smolin, Quantum-channel capacity of very noisy channels, Phys. Rev. A **57**, 830 (1998).

[58] K. Fukui, A. Tomita, and A. Okamoto, Analog Quantum Error Correction with Encoding a Qubit into an Oscillator, Phys. Rev. Lett. **119**, 180507 (2017).

[59] D. Poulin, Optimal and efficient decoding of concatenated quantum block codes, Phys. Rev. A **74**, 052333 (2006).

[60] T. C. Ralph, A. J. F. Hayes, and A. Gilchrist, Loss-Tolerant Optical Qubits, Phys. Rev. Lett. **95**, 100501 (2005).

[61] S. Muralidharan, J. Kim, N. Lütkenhaus, M. D. Lukin, and L. Jiang, Ultrafast and Fault-Tolerant Quantum Communication Across Long Distances, Phys. Rev. Lett. **112**, 250501 (2014).

[62] W. J. Munro, A. M. Stephens, S. J. Devitt, K. A. Harrison, and K. Nemoto, Quantum communication without the necessity of quantum memories, Nat. Photonics **6**, 777 (2012).

[63] F. Ewert, M. Bergmann, and P. van Loock, Ultrafast Long-Distance Quantum Communication with Static Linear Optics, Phys. Rev. Lett. **117**, 210501 (2016).

[64] A. M. Steane, Active Stabilization, Quantum Computation, and Quantum State Synthesis, Phys. Rev. Lett. **78**, 2252 (1997).

[65] B. W. Walshe, B. Q. Baragiola, R. N. Alexander, and N. C. Menicucci, Continuous-variable gate teleportation and bosonic-code error correction, Phys. Rev. A **102**, 062411 (2020).

[66] E. Knill, Scalable quantum computing in the presence of large detected-error rates, Phys. Rev. A **71**, 042322 (2005).

[67] S. Glancy and E. Knill, Error analysis for encoding a qubit in an oscillator, Phys. Rev. A **73**, 012325 (2006).

[68] See Supplemental Material at http://link.aps.org/supplemental/10.1103/PhysRevLett.131.170603 for details

of the quantum error correction for the parity code with our method.

[69] C. Chamberland and T. Jochym-O'Connor, Error suppression via complementary gauge choices in Reed-Muller codes, Quantum Sci. Technol. **2**, 035008 (2017).

[70] D. K. Tuckett, Tailoring surface codes: Improvements in quantum error correction with biased noise, Ph.D. thesis, The University of Sydney, Sydney, 2020.

[71] M. Varnava, D. E. Browne, and T. Rudolph, Loss Tolerance in One-Way Quantum Computation via Counterfactual Error Correction, Phys. Rev. Lett. **97**, 120501 (2006).

[72] S. D. Barrett and T. M. Stace, Fault Tolerant Quantum Computation with Very High Threshold for Loss Errors, Phys. Rev. Lett. **105**, 200502 (2010).

[73] J.-P. Tillich and G. Zémor, Quantum LDPC codes with positive rate and minimum distance proportional to the square root of the blocklength, IEEE Trans. Inf. Theory **60**, 1193 (2013).

[74] J. P. Bonilla Ataides, D. K. Tuckett, S. D. Bartlett, S. T. Flammia, and B. J. Brown, The XZZX surface code, Nat. Commun. **12**, 2172 (2021).

[75] L. Hänggli, M. Heinze, and R. König, Enhanced noise resilience of the surface–Gottesman-Kitaev-Preskill code via designed bias, Phys. Rev. A **102**, 052408 (2020).

[76] M. P. Stafford and N. C. Menicucci, Biased Gottesman-Kitaev-Preskill repetition code, arXiv:2212.11397.